Journal of the European Ceramic Society 23 (2003) 481–489

www.elsevier.com/locate/jeurceramsoc

Transformation-induced damping behaviour of Y-TZP zirconia ceramics

G. Roebben*, B. Basu[1], J. Vleugels, O. Van der Biest

Department of Metallurgy and Materials Engineering, Katholieke Universiteit Leuven, Kasteelpark Arenberg 44, B-3001 Heverlee, Belgium

Received 8 December 2001; accepted 8 April 2002

Abstract

Stiffness and internal friction of yttria-stabilised tetragonal zirconia ceramics (Y-TZP) with varying yttria content (2–3 mol%) were measured between room temperature and 1000 K with the use of the impulse excitation technique (IET). The contribution of transformation-related damping events to internal friction is recognised and separated from damping due to elastic dipole relaxation. Damping effects associated with tetragonal-to-monoclinic and reversed ZrO_2-phase transformation and low temperature degradation (LTD), are identified with the help of dilatometry. The experimental results indicate that 2Y-TZP with an inhomogeneous yttria distribution shows controlled transformation induced damping behaviour and less susceptibility to LTD during thermal cycling compared to a co-precipitated 2Y-TZP material with homogeneous Y-distribution.

Keywords: Internal friction; Mechanical spectroscopy; Structural applications; Thermal expansion; Toughening; ZrO_2

1. Introduction

In pure ZrO_2, a volume expanding tetragonal-to-monoclinic (t→m) phase transformation occurs spontaneously during cooling below 1170 °C. Therefore, undoped ZrO_2 ceramics disintegrate during cooling from the sintering temperature. It is now well known that the tetragonal zirconia can be retained at room temperature through the addition of stabilising oxides, which introduces aliovalent cations into the ZrO_2 lattice. In this paper yttria-stabilised tetragonal ZrO_2 (Y-TZP) will be discussed, with xY-TZP corresponding to TZP stabilised with x mol% of Y_2O_3 additives. Depending on the type, amount and distribution of stabilising dopants and the concomitant ZrO_2 grain size, the tetragonal zirconia transforms to the monoclinic phase in particular circumstances of temperature, stress and/or humidity .[1,2] Since the chemical driving force for the stress-free, athermal, martensitic t→m transformation increases with decreasing temperature, the transformation can be induced by cooling below M_s, the onset temperature of the martensitic transformation. Alternatively the volume-expanding t→m transformation can be induced in the tensile stress field around a crack tip. For a crack growing under load, the transformation results in a zone of higher monoclinic concentration in the crack wake. The volume expansion induces a closing action in the crack wake and decreases the stress intensity experienced at the crack-tip. This so-called 'phase transformation toughening' effect is the origin of high mechanical reliability of ZrO_2 materials .[3]

For increased fracture toughness, the tetragonal phase transformability is the critical factor. The key is to maximise the retention of tetragonal zirconia at room temperature or application temperature with sufficient transformability in a tensile stress field. This issue is strongly affected by low-temperature-degradation (LTD).[4] LTD is the progressive transformation of critically stabilised tetragonal zirconia to monoclinic during ageing at relatively low temperatures, typically between 100 and 300 °C. With increasing temperature to 400 °C or more, the thermodynamic driving force for the t→m-transformation decreases, and LTD is arrested. LTD is reported to be more severe in humid environments. Different microstructural parameters influencing LTD are reported in the existing literature .[4]

* Corresponding author. Tel.: +32-16-321192; fax: +32-16-321992.

E-mail address: gert.roebben@mtm.kuleuven.ac.be (G. Roebben).

[1] Presently Assistant Professor, Department of Materials and Metallurgical Engineering, Indian Institute of Technology (IIT), Kanpur 208016, India.

0955-2219/02/$ - see front matter
PII: S0955-2219(02)00101-2

In this perspective, it is important to explore the experimental methods that enable characterising the t→m-transformation. Since the transformation is accompanied by a volume expansion, dilatometry is an effective experimental tool. In recent times, detailed dilatometry experiments were performed in our laboratory to investigate the tetragonal zirconia transformation in different grades of ZrO_2–TiB_2 composites .[5] Another way to characterise the transformation is mechanical spectroscopy, i.e. the measurement of stiffness and/or internal friction or damping (Q^{-1}) as a function of e.g. temperature.[6] Monitoring the change of elastic and anelastic properties with temperature provides a sensitive tool for the detection of subtle microstructural events. Recently, Basu et al.[7] were the first to demonstrate that the t→m transformation in 2Y-TZP is accompanied by an increase in damping, as measured using a torsion pendulum. This calls for a detailed investigation into the damping behaviour of this class of structural ceramics.

Another characteristic feature of the internal friction behaviour of TZP ceramics is the evolution of a damping peak at around 200 °C .[8] Shimada et al. initially attributed this peak to the motion of twin boundaries in monoclinic ZrO_2 grains. Later on, the same authors corrected their view and provided the evidence linking the damping peak with stress induced oxygen movement both in 2Y-TZP and 3Y-TZP .[9] Following this, Weller has presented a detailed atomistic model and full characterisation of this peak.[10] The appearance of the damping peak is due to the movement of oxygen vacancies around immobile yttrium substitutional atoms. Since the oxygen vacancies and associated yttrium substitutional ions form an elastic dipole (Y'_{Zr} V''_O), their energy depends on the orientation of the applied stress. When sufficient thermal activation energy is provided, the oxygen vacancies will react to an applied stress by moving to a position of minimum strain energy. This relaxation effect is characterised by a temperature dependent relaxation time. Applying a cyclic load with a period equal to this relaxation time brings about the maximum damping. The maximum damping value is related to the amount of Y^{3+} ions in the ZrO_2-lattice.

In the present work, the impulse excitation technique (IET) has been employed to determine the stiffness and damping behaviour of several Y-TZPs. In IET, a test sample is excited by a gentle impulse, to induce resonance frequencies of the test sample, typically within a frequency range between 50 Hz and 50 kHz. The resonance frequencies are related to the stiffness of the material. The decay of the vibration amplitude is related to the damping or internal friction of the material. Since modern IET-tools register with a high accuracy the change of stiffness and damping as a function of temperature,[11] such equipment was used to obtain detailed information on the t→m transformation.

2. Materials and experimental procedure

2.1. Materials

Zirconia starting powders used in the present investigation include 3 mol% yttria co-precipitated powders (Tosoh grade TZ-3Y and Daiichi grade HSY-3U) and yttria-free monoclinic zirconia powders (Tosoh grade TZ-0). Co-precipitated powder, as well as mixtures of 3 mol% co-precipitated powder and Y-free monoclinic powder, were hot pressed in boron nitride coated graphite dies, at 1450 °C for 1 h in vacuum (≈0.1 Pa) under a mechanical load of 28 MPa. A range of Y-TZP ceramics with an overall Y_2O_3–content of 2 mol% (TM2 and DM2), 2.5 mol% (TM2.5) and 3 mol% (T3) were obtained. The T3 grade is made from TZ-3Y powder. Among the mixed ceramics, TM grades are processed from the powder mixture of TZ-3Y and TZ-0, whereas DM grades are from HSY-3U and TZ-0. The powder mixing is carried out in a polyethylene bottle in ethanol using alumina-milling medium. Due to the use of an alumina milling-medium during powder mixing, small amounts of alumina were incorporated in the TM and DM ceramics. ICP analysis revealed the presence of 0.40–0.45 wt.% Al_2O_3 in the TM2.5 and TM2 ceramics, 0.2 wt.% in the DM ceramic, whereas the alumina content in the T3 grade is 0.02 wt.%. Some microstructural and mechanical properties of the tested materials, taken from[12] are summarised in Table 1. The density and the hardness data implicate that the investigated Y-TZPs are fully dense. Looking at Table 1, it is also clear that the intentional addition of the monoclinic zirconia particles to 3 mol% yttria stabilised powders increases the grain growth and the indentation toughness. The strength values around 1 GPa, as obtained with the investigated ceramic grades are typically representative data of the dense Y-TZPs. In the TM- and DM-grade ceramics, an inhomogeneous Y-distribution is observed compared to the homogeneous yttria distribution measured in the T3 ceramic.[12] HRTEM investigation carried out in our laboratory could not reveal the presence of any continuous grain boundary phase in the hot pressed microstructure.[12]

Table 1
Microstructural and mechanical properties of the investigated Y-TZP materials[12]

Ceramic grades	m-ZrO_2 content[a] (vol.%)	Mean grain size (μm)	HV_{10} (GPa)	E (GPa)	Density (kg/dm^3)	3-Point flexural strength[b] (MPa)	K_{IC} (10 kg) (MPa m$^{1/2}$)
T3	0	0.31	11.9±0.2	194	6.08	1007±126	2.5±0.1
TM2.5	0	0.35	12.6±0.1	203	6.05	1085±35	5.7±0.1
TM2	2.7	0.49	11.9±0.1	215	6.04	1269±150	10.3±0.5
DM2	2.7	0.50	11.5±0.2	214	6.00	1257±114	10.1±0.5

[a] As measured by X-ray diffraction on polished samples.
[b] Span between outer loading points = 20 mm, nominal sample size 25 × 5 × 2 mm^3.

2.2. Impulse excitation technique (IET)

The non-destructive impulse excitation technique (IET) is a standard test method for the determination of dynamic elastic moduli of materials at room temperature [ASTM E 1876–97,[13] ENV 843–2[14]]. In this paper, data obtained with a digital signal analysis based IET-device are presented. The sound of the vibrating beam-like sample, captured and transformed into an electric signal by a microphone, is digitised and analysed by the RFDA-software (IMCE, Diepenbeek, Belgium) as described in.[11] The program defines a function of the form $x(t) = x_0\, e^{-kt} \sin(2\pi f_r t + \phi)$ for a chosen maximum number of resonance frequencies. An algorithm simulates the measured signal as a sum of these transient sinusoidal waves, optimising in an iterative manner the parameters x_0, k, f_r and ϕ. The elastic moduli are calculated from the flexural resonance frequency f_f using the relations prescribed by ASTM E 1876–97 and ENV 843–2. The corresponding Q^{-1} is calculated as $Q^{-1} = k/(\pi f_f)$.[11]

In the present investigation, IET data are obtained at elevated temperatures. The experiments were performed in a purpose-built IET-furnace (J.W.Lemmens, Leuven, Belgium), the core of which is schematically presented in Fig. 1. In the IET-furnace, the sample is suspended by two wires that are stretched in planes perpendicular to the long axis of the sample. The wires follow a trajectory between parallel Al_2O_3-rods attached to the front-flange of the furnace. Each of the wires holds the test sample at one of the two nodes of the bar's fundamental flexure vibration mode. The wires are made of NiCr, enabling tests up to 1400 K in air. Once inserted in the furnace, the sample finds itself in-between two hollow tubes. Through a first tube, arriving from below, a small ceramic cylinder is pneumatically fired. The projectile drops back in the pneumatic channel after impact. The second tube comes from above and serves as an acoustic wave-guide, leading the sound of the vibrating sample to a microphone, placed outside the furnace.

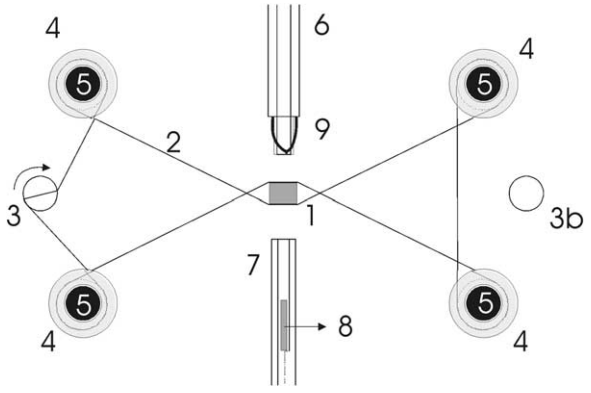

Fig. 1. Front-view of the impulse excitation set-up in the J.W.Lemmens IET-furnace. (1) Test sample. (2) 1 of 2 NiCr-wires, which support the sample in one of the nodes of the flexure vibration mode. (3) Al_2O_3 bars linked to a stepping motor, which is empowered periodically to turn the bars and prevent the sample from moving down as the NiCr wire thermally expands or creeps. (3b) Rotating bar to fix the second wire, supporting the sample at the second node of the flexure mode (not shown). (4) Short Al_2O_3 cylinders that can move along and rotate around the Al_2O_3 bars (5) fixed to the furnace front flange. (6) Hollow Al_2O_3 tube leading the sound of the excited sample out of the furnace to a microphone. (7) Hollow Al_2O_3 tube through which the Al_2O_3 projectile (8) is fired pneumatically at the sample. (9) Thermocouple.

IET tests were carried out on bars of Y-TZP, machined from the hot-pressed disks. The test samples have a rectangular cross-section and a nominal length of 40 mm. Tests were run between room temperature and 1000 K. Data were collected during heating and cooling stages (2 K/min) of up to three thermal cycles.

2.3. Subtraction of the damping due to elastic dipole relaxation

Fig. 2 shows the stiffness and damping of the DM2 ceramic during two thermal cycles. An internal friction peak near 490 K dominates the spectrum. Associated with the damping peak is a relaxation of the Young's modulus. At about 750 K, a second damping feature can be discerned. Whereas the former peak is rather stable during heating and cooling in successive thermal cycles, the second peak is seen to depend on the thermal history of the sample. Similar tests were performed on the other Y-TZP ceramics. In each case, a damping peak is observed near 490 K.

The occurrence of the peak at 490 K is well-documented[15–17] and is due to the elastic dipole relaxation, as described in the introduction. To better discern the other damping features, the damping due to the dipole relaxation peak was subtracted from the measured internal friction data. The deconvolution of damping data needs to be done with appropriate care[18] and in fact can only be successfully performed for well-defined damping phenomena. As this is the case for the elastic dipole peak, it was decided to fit its shape by the commonly proposed broadened Debye peak,[19] taking all parameters that determine the shape of the peak from

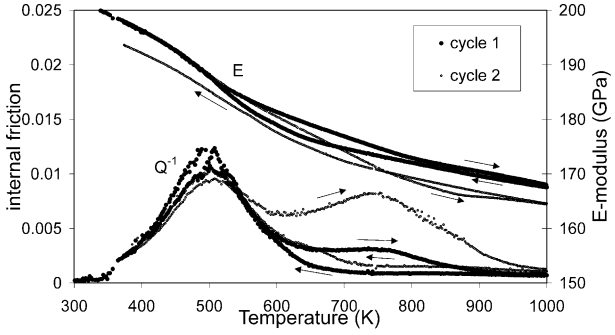

Fig. 2. Stiffness and damping of the DM2 ceramic in two successive thermal cycles between room temperature and 1000 K; resonance frequency at 300 K = 8100 Hz.

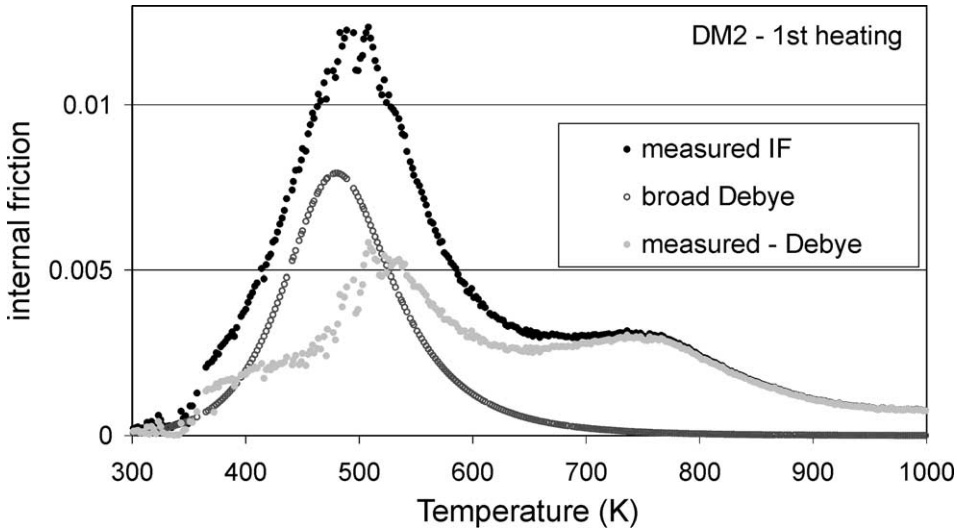

Fig. 3. Internal friction in DM2 during the first heating stage. The experimental data are shown together with the calculated elastic dipole peak, and the difference between the measured and the calculated data.

an independent source.[16] According to Weller[16] and others,[9,15] the activation energy of the dipole relaxation peak equals 90 kJ/mol. According to the results of Weller, the relaxation strength Δ, determining the height of the peak ($\Delta = 2 \times Q_{max}^{-1}$), varies linearly with the amount of Y_2O_3-additives ($\Delta = 0.008 \times$ mol% Y_2O_3). This linear relation cannot be extrapolated beyond 3 mol% Y_2O_3, as Weller has shown how an increase in Y_2O_3 content results in the formation of satellite peaks, indicative of larger agglomerates of yttrium ions with oxygen vacancies.[16] Agglomeration is reported to aggravate by long-term ageing at 800 °C, and noticeably decreases the relaxation Q^{-1}-peak, even for 2Y-TZP.[20] The broadening factor of the Debye peak is set equal to 2. Again this reflects Weller's observation that the FWHM of the elastic dipole peak is two times that of a Debye peak, when plotted in a Q^{-1} vs. $1/T$ plot.

The position of the fitted peak along the temperature axis was adjusted for each sample individually. Hence, the peak temperature is the only fitting parameter. The soundness of the fitting procedure can be judged from the limit relaxation time, which was calculated from the measured resonance frequency at the peak temperature, the given activation energy and the fitted peak temperature (Table 2). This parameter is highly similar for all the tested samples (3.2 10^{-15} s), which compares well with literature values.[16,21]

Having calculated the elastic-dipole damping-peak, it was subtracted from the measured damping data. This is illustrated in Fig. 3 for the DM2 ceramic, during the first heating stage. For this particular heating stage, as well as for most other tests, a distinct damping feature is revealed in the neighbourhood of the elastic-dipole peak. The difference between measured damping and the calculated damping now can be related to damping phenomena other than the elastic dipole relaxation. The interpretation of the residual damping values is based on a comparison with the results of the dilatometry tests.

2.4. Dilatometry measurements

Dilatometry tests were performed on Y-TZP samples machined out of hot pressed discs. The sample's nominal height was 9 mm and the uniform cross-section measured 5 × 5 mm. The thermal expansion was measured in air from room temperature up to 1050 K, using a commercial dilatometer (model TMA 800, Dupont 943, USA). Each specimen was subjected to up to three thermal cycles.

Table 2
Experimentally determined and calculated parameters describing the shape and position of the elastic dipole peak

Ceramic grades	Y_20_3-content (mol%)	Peak temperature (K)	Peak frequency (Hz)	Relaxation strength (−)	FWHM (K)	Limit relaxation time (10^{-15} s)
T3	3	478	7185	0.024	134	3.24
TM2.5	2.5	475	6295	0.020	133	3.20
TM2	2	492	14359	0.016	142	3.23
DM2	2	480	7861	0.016	133	3.25

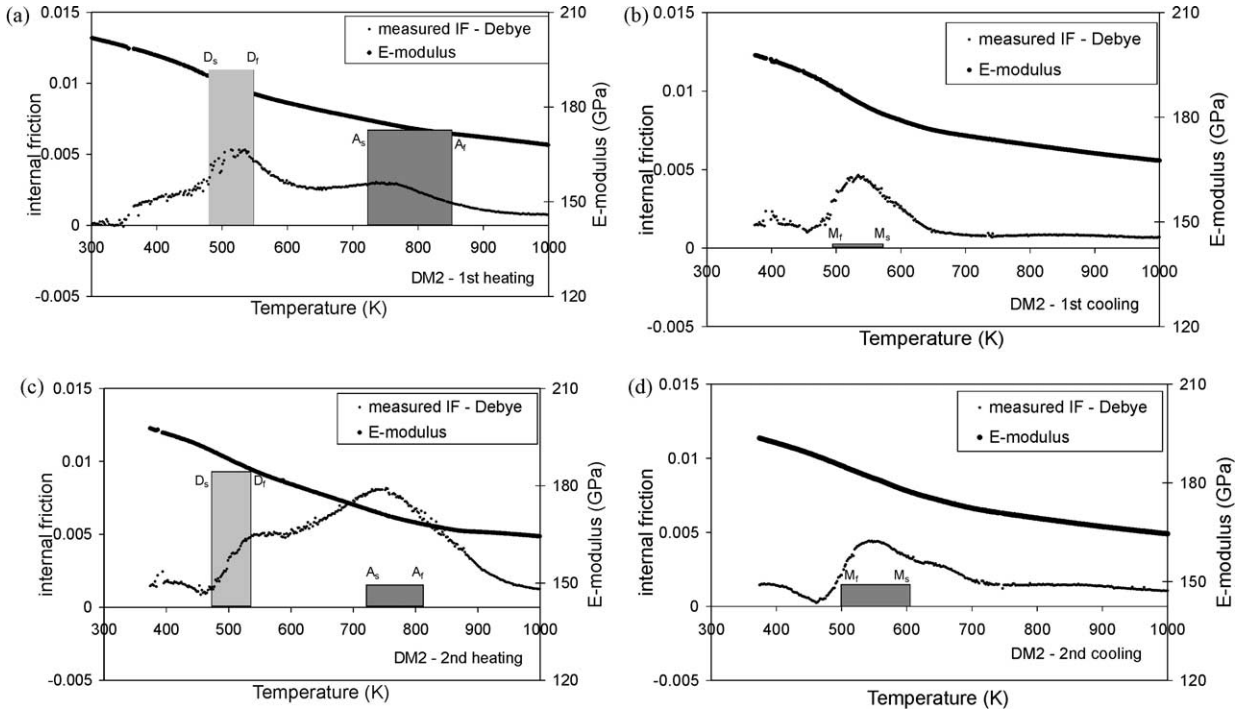

Fig. 4. Stiffness and residual damping (=measured damping-elastic dipole contribution) for the DM2 ceramic; (a) first heating stage, (b) first cooling stage, (c) second heating stage, (d) second cooling stage. Shaded areas indicate the temperature range over which dilatometry has revealed anomalous thermal expansion and shrinkage effects (D=low-temperature degradation, M=martensitic transformation, A=austenitic transformation, subscripts s and f=start and finish temperature, respectively). The height of the shaded area corresponds with the intensity of the measured thermal expansion/shrinkage.

3. Results

3.1. Damping and thermal expansion in 2Y-TZP with heterogeneous Y-distribution

Fig. 4 shows the residual damping (=measured damping-elastic dipole contribution) in the DM2 material, and the variation of the E-modulus, during the four consecutive temperature stages. Superimposed on the graphs in Fig. 4 are shaded areas, which indicate the temperature range in which dilatometry tests have revealed anomalous thermal expansion/contraction. The deduction of the lower and higher ends of these temperature ranges from the raw thermal expansion and shrinkage data has been described in,[5] and follows traditional definitions of start (M_s, A_s) and end (M_f, A_f) temperatures of martensitic and reverse (austenitic) transformations. D_s and D_f denote the onset and finish temperature of low temperature degradation upon heating.

3.2. t→m-Transformation in samples with different Y-content and distribution

IET-tests were attempted on Y-TZP materials with a homogeneous yttria distribution prepared from 2 mol% co-precipitated ZrO_2 (Tosoh grade TZ-2Y). Whereas these materials can be investigated with dilatometry, as presented in Ref. [7], it should be noted that more than one thermal cycle in a dilatometry test with TZ-2Y grade was not possible earlier due to extensive microcracking, induced by the tetragonal phase transformation. In the present study, the bars made of TZ-2Y ceramic grade did not possess the required structural soundness to undergo the impulse excitation tests. More specifically, when the IET test reaches the LTD-temperature range, the TZ-2Y samples progressively degrade under the repeated impulse excitation, and break up into small pieces. Earlier torsion pendulum tests on 2Y-TZP materials did succeed in measuring Q^{-1} in a single heating stage up to elevated temperature.[21] In our earlier study, a torsion pendulum test was performed on the identical TZ-2Y grade for one full thermal cycle.[7] In this sense, IET-tests are currently less forgiving for structural deterioration of the test sample. Fig. 5 presents an overview of the stiffness and internal friction IET-data obtained during the first thermal cycle on four successfully investigated Y-TZP materials (T3, TM2.5, TM2 and DM2). The fact that the Y-TZP materials with a heterogeneous Y-distribution (TM and DM grades) withstand the thermal cycles as well as the repeated mechanical impulse excitation, is another confirmation of the structural quality of these materials in addition to their room temperature fracture toughness and flexural strength values (Table 1).

4. Discussion

4.1. Interpretation of the thermal expansion events

The interpretation of the thermal expansion events presented earlier[5,7,12] is briefly summarised here for reasons of clarity. The particular thermal expansion phenomenon observed during heating around 500 K [Fig. 4(a) and (c)], corresponds with the so-called low-temperature-degradation (LTD). LTD is caused by the volume-expanding transformation of the metastable tetragonal phase to the stable monoclinic phase in critically stabilised Y-TZP. LTD is known to occur under conditions of ageing at low temperature, between D_s and D_f, the start and finish temperatures graphically indicated in Fig. 4.

When heating to about 800 K, an anomalous contraction of the material is observed, due to the reverse transformation from monoclinic to tetragonal phase. The transforming monoclinic phase was formed at lower temperatures during cooling after sintering, or due to LTD. During cooling between M_s and M_f, the anomalous thermal expansion is observed and is related to the martensitic transformation of the tetragonal to the monoclinic phase.

4.2. Comparison of thermal expansion and damping events

From Fig. 4(a)–(d), one observes a close agreement between the temperature range in which damping increases (IET) and the temperature range of anomalous thermal expansion/contraction (dilatometry). This is a strong evidence for an association of the damping events to the same microstructural phenomena causing the thermal expansion anomalies, i.e. the forward and reverse martensitic transformations causing damping. During heating, LTD and reverse transformation contribute to an increased damping. Also, the martensitic t→m transformation is responsible for a damping maximum during the cooling stages.

The above interpretation of the IET-damping results agrees with the conclusions of a previous mechanical spectroscopy study in which damping in homogeneous 2Y-TZP was determined with torsion pendulum tests.[7] The frequency applied in the torsion pendulum tests is of the order of 1 Hz. This reduces the temperature at which the relaxation peak occurs. Since the temperature at which phase-transformations induce damping is independent of the applied frequency, this results in a clear separation of the twofold contribution to internal friction in the low temperature regime (100–300 °C), one being due to elastic dipole relaxation and the other to phase transformation. Actually, with the knowledge obtained from these torsion pendulum tests and the IET-tests presented in this paper, both contributions can now be recognised a posteriori in earlier published experimental results.[22–25] Indeed, in these papers the high temperature foot of the elastic dipole peak is stretched out, due to what we now understand is the

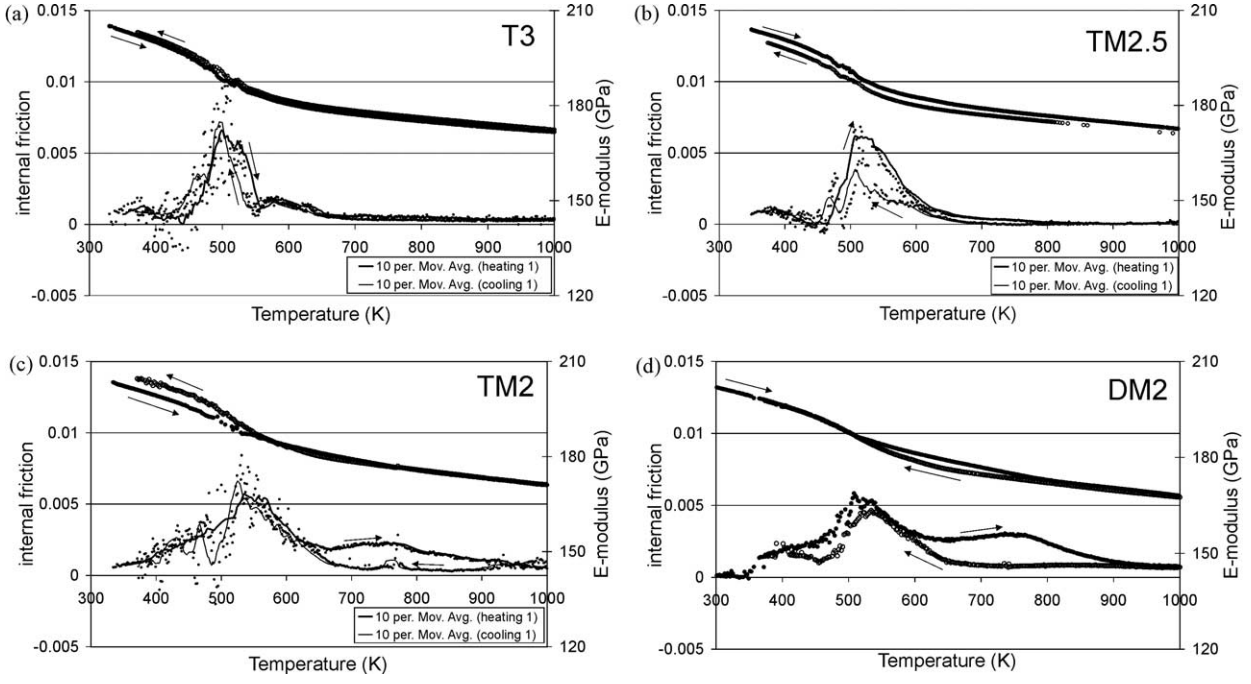

Fig. 5. Comparison of the stiffness and residual internal friction (after subtraction of the elastic dipole damping from the measured IET data) for the four investigated Y-TZP-materials: 3Y-TZP (a), 2.5Y-TZP (b) and 2Y-TZPs (c and d), during the first thermal cycle.

damping due to LTD upon heating, or martensitic t→m-transformation upon cooling.

In an attempt to correlate the height of the damping peak with the extent of the thermal expansion, the height of the shaded areas in Fig. 4 has been chosen proportional to the absolute value of the linear expansion. The dilatometry data are taken from.[5] The data in Fig. 4(a) suggest that there is a correlation between the intensity of the thermal expansion jump and the height of the associated damping peak. On the other hand, the thermal expansion associated with the damping event in the first cooling stage is rather small. Nevertheless, the height of the damping peak is of the same order as that observed during heating in the same temperature range. The damping behaviour during the second thermal cycle is different from the first. While the damping associated with LTD remains similar to that observed in the first thermal cycle, a considerably more intense damping level is reached in the reverse transformation temperature range. This is in disagreement with the trends observed in the thermal expansion volume. The same disagreement is seen in the results obtained in the second cooling stage, in which the martensitic transformation is detected again [Fig. 4(d)]. While the associated thermal expansion has become more important, the damping has remained the same. The results provide no evidence for a straightforward relation between the thermal expansion volume and the height of the internal friction peak. Microcracking is suspected to be one of the reasons for this observation. Microcracks develop in the ZrO_2 microstructure upon every t→m or reverse transformation.[2] Once a microcrack is nucleated, it is unlikely that the microcracks will disappear during the imposed IET-thermal cycles. The damping effects of cracks in a single sample will therefore develop and increase with the number of thermal cycles. Not only will this affect the background damping in between particular transformation associated damping events [compare Fig. 4(b) and (d)], microcracks are also expected to influence the ease of transformation. This is assumed to be the reason for different damping intensities associated with similar transformation events in consecutive thermal cycles, and remains to be investigated further.

4.3. Internal friction of Y-TZP grades with homogeneous and heterogeneous Y-distribution

From Fig. 5, a clear impression is obtained of the increase of the transformation intensity with decreasing amount of stabilising Y_2O_3 additives. The amount of Y_2O_3 additives is observed to be a dominating factor. Similar damping behaviour is recorded in the mixed 2Y-TZP grades (DM2 versus TM2) processed from different starting powders (Tosoh and Daiichi powders). Most interesting is the fact that the 2Y-TZP materials with heterogeneous Y-distribution (DM2 and TM2) withstand up to three thermal IET-test cycles. This distinguishes them from the homogeneous 2Y-TZP, which consistently broke during the first IET cycle. This indicates DM2 and TM2 ceramics undergo a more constrained and more localised transformation throughout their microstructure. This can explain the high level of reversibility of the transformation events observed in consecutive IET-tests (Fig. 4).

In comparison to the torsion pendulum test results obtained on a homogeneous 2Y-TZP material,[7] the behaviour of the heterogeneous 2Y-TZP materials shown in Figs. 2–5 is different. Whereas homogeneous 2Y-TZP shows well-defined narrow Q^{-1}-peaks in a temperature scan, an almost steady-state damping level is maintained for heterogeneous 2Y-TZP in between the LTD and reverse t→m-transformation temperature regimes. This can be a direct result of the heterogeneous Y_2O_3-distribution. Since LTD and reverse transformability of individual grains depend a.o. on the local Y_2O_3-content, a broad distribution of transformation events is expected when heating heterogeneous materials.

4.4. Outlook

It is understood that martensitic phase transformations are associated with the movement of phase boundaries, which dissipates energy.[26,27] Liu and Chen[28] suggest a thermally activated double kink process to be the origin of the mobility of the t/m-interface. According to,[29] loading–unloading sequences multiply the nucleation sites for transformation. The IET-results in Fig. 4 suggest the same applies for repeated thermal loading/unloading with an increase in transformation events in consecutive thermal cycles. However, lacking in this discussion is the detailed microstructural origin of the damping contribution linked with the t→m-transformations. This subject remains to be further investigated. Also, the effect of the Al_2O_3 content in different Y-TZP grades is currently under investigation, as it is reported to reduce the susceptibility of tetragonal phase transformation.[29]

A final remark can be made on the high damping capacity of the TZP ceramics in the temperature range of martensitic transformation. This behaviour has implication as far as the structural applications of the transformation-toughened ceramics are concerned. The reduction of unwanted vibration of structural components can be realised with the use of TZP ceramics, thus improving the life of the ceramic in technological applications. In this respect, the broad temperature range of increased damping capacity in the 2Y-TZP samples with heterogeneous Y-distribution is more desirable than the earlier reported isolated damping peaks observed in 2Y-TZP with a homogeneous Y-distribution.[7]

5. Conclusions

In the present study, IET is shown to be a powerful technique for characterising the damping features caused by LTD, forward and reverse martensitic transformation in Y-TZP materials. To effectively discern the transformation-associated damping events, a peak deconvolution procedure is presented allowing subtracting the damping contribution of the elastic dipole relaxation peak from the measured IET data. Dilatometry and IET data exhibit close correspondence in describing the transformation behaviour of the investigated TZP ceramics. In comparison with other mechanical spectroscopy techniques, the IET technique is less forgiving with respect to the structural degradation of weakly stabilised Y-TZP materials during LTD. As such, the IET-tests have shown that the low-temperature structural degradation is significantly improved in 2Y-TZP ceramics with inhomogeneous Y-distribution compared to that with homogeneous Y-distribution. A high reversibility of the t→m-transformation in the heterogeneous materials is deduced from the results of consecutive thermal cycles of IET-tests. The results provide evidence for constrained, less degrading transformation events in Y-TZP with a heterogeneous Y-distribution.

Acknowledgements

G. Roebben thanks the Fund for Scientific Research, Vlaanderen (FWO) for his research fellowship. B. Basu thanks the K.U. Leuven Research Council for his fellowship. This work was partially supported by the Flemish Region, IWT.

References

1. Hannink, R. H. J., Kelly, P. M. and Muddle, B. C., Transformation toughening in Zirconia-containing ceramics. *J. Am. Ceram. Soc.*, 2000, **83**, 461–487.
2. Ruhle, M. and Evans, A. G., High toughness ceramics and ceramic composites. *Prog. Mater. Sci.*, 1989, **33**, 85–167.
3. Garvie, R. C., Hannink, R. H. J., and Pascoe, R. T., Ceramic steel? Nature., 1975, **258**, 703.
4. Lawson, S., Review: environmental degradation of zirconia ceramics. *J. Eur. Ceram. Soc.*, 1995, **15**, 485–502.
5. Basu, B., Vleugels, J. and Van der Biest, O., Transformation behaviour of yttria stabilized tetragonal zirconia polycrystal - TiB_2 composites. *J. Mater. Res.*, 2001, **16**, 2158–2169.
6. Roebben, G., Basu, B., Vleugels, J., Van Humbeeck, J. and Van der Biest, O., The innovative impulse excitation technique for high temperature mechanical spectroscopy. *J. Alloys Compounds*, 2000, **310**, 284–287.
7. Basu, B., Donzel, L., Van, Humbeeck, J., Vleugels, J., Schaller, R. and Van der Biest, O., Thermal expansion and damping characteristics of Y-TZP. *Scripta Mater.*, 1999, **40**, 759–765.
8. Shimada, M., Matsushita, K., Kuratani, S., Okamoto, T., Koizumi, M., Tsukuma, K. and Tsukidate, T., Temperature dependence of Young's modulus and internal friction in alumina, silicon nitride, and partially stabilized zirconia ceramics. *J. Am. Ceram. Soc.*, 1984, **67**, C-23–C-24.
9. Matsushita, K., Okamoto, T. and Shimada, M., Internal friction in partially stabilized zirconia. *J. Phys., Colloque C10*, 1985, **46**, 549–552.
10. Weller, M. and Schubert, H., Internal friction, dielectric loss, and ionic conductivity of tetragonal ZrO_2–3% Y_2O_3 (Y-TZP). *J. Am. Ceram. Soc.*, 1986, **69**, 573–577.
11. Roebben, G., Bollen, B., Brebels, A., Van Humbeeck, J. and Van der Biest, O., Impulse excitation apparatus to measure resonant frequencies, elastic moduli, and internal friction at room and high temperature. *Rev. Sci. Instrum*, 1997, **68**, 4511–4515.
12. Basu, B., *Zirconia-titanium Boride Composites for Tribological Applications*. PhD thesis. Katholieke Universiteit Leuven, 2001.
13. Standard Test Method for Dynamic Young's Modulus, Shear Modulus, and Poisson's Ratio by Impulse Excitation of Vibration E 1876 – 97, American Society for Testing and Materials, West Conshohocken, PA, 1998.
14. Advanced Technical Ceramics—Monolithic Ceramics, Mechanical Properties at Room Temperature—Part 2: Determination of Elastic Moduli. ENV 843–2, European Committee for Standardisation, Brussels, 1995.
15. Lakki, A., *Mechanical Spectroscopy of Fine-Grained Zirconia, Alumina and Silicon Nitride*. PhD thesis, Ecole Polytechnique Fédérale, Lausanne, 1994.
16. Weller, M., Schubert, H. and Kountouros, P., 1993. Mechanical and dielectric loss measurements in Y_2O_3–ZrO_2 and TiO_2–Y_2O_3–ZrO_2 ceramics. In *Science and Technology of Zirconia V*, ed. Badwal, S. P. S., Bannister, M. J. and Hannink, R. H. J. Technomic Publ. Co., Lancaster and Basel, pp. 546–554.
17. Weller, M., 2001. Point defect relaxations. In *Mechanical Spectroscopy Q^{-1} 2001, Materials Science Forum*, ed. Schaller, R., Fantozzi, G. and Gremaud, G. Vols. 366–368. Trans Tech Publications, Zürich, Switzerland, pp. 95–140.
18. San Juan, J., 2001. Mechanical spectroscopy. In *Mechanical Spectroscopy Q^{-1} 2001, Materials Science Forum*, ed. Schaller, R., Fantozzi, G. and Gremaud, G. Vols. 366–368. Trans Tech Publications, Zürich, Switzerland, pp. 32–73.
19. Fantozzi, G., 2001. Phenomenology and definitions. In *Mechanical Spectroscopy Q^{-1} 2001, Materials Science Forum*, ed. Schaller, R., Fantozzi, G. and Gremaud, G. Vols. 366–368. Trans Tech Publications, Zürich, Switzerland, pp. 3–31.
20. Kondoh, J., Kikuchi, S., Tomii, Y. and Ito, Y., Effect of aging on yttria-stabilized zirconia, III. A study of the effect of local structures on conductivity. *J. Electrochem. Soc.*, 1998, **145**, 1550–1560.
21. Lakki, A., Schaller, R., Nauer, M. and Carry, C., High temperature superplastic creep and internal friction of yttria doped zirconia polycrystals. *Acta Metall. Mater.*, 1993, **41**, 2845–2853.
22. Weller, M., Atomic defects in yttria- and calcia-stabilised zirconia. *Z. Metallkd*, 1993, **84**, 381–386.
23. Sakaguchi, S., Wakai, F. and Matsuno, Y., Elastic properties of engineering ceramics at elevated temperatures. *J. Ceram. Soc. Jpn. Int. Ed.*, 1987, **95**, 429–432.
24. Ono, T., Nurishi, Y., Hashiba, M. and Tanahashi, K., Temperature dependence of internal friction in Al_2O_3–3Y–ZrO_2 composites. *J. Mater. Sci. Lett.*, 1989, **8**, 569–570.
25. Nishiyama, K., Yamanaka, M., Omori, M. and Umekawa, S., High-temperature dependence of the internal friction and modulus change of tetragonal ZrO_2, Si_3N_4 and SiC. *J. Mater. Sci. Lett.*, 1990, **9**, 526–528.
26. Van Humbeeck, J., 2001. The martensitic transformation. In *Mechanical Spectroscopy Q^{-1} 2001, Materials Science Forum*, ed.

Schaller, R., Fantozzi, G. and Gremaud, G. Vols. 366–368. Trans Tech Publications, Zürich, Switzerland, pp. 382–415.
27. Van Humbeeck, J., Stoiber, J., Delaey, L. and Gotthardt, R., The high damping capacity of shape memory alloys. *Z. Metal*, 1995, **86**, 176–183.
28. Liu, S.-Y. and Chen, I-W., Fatigue deformation mechanisms of zirconia ceramics. *J. Am. Ceram. Soc.*, 1992, **75**, 1191–1204.
29. Grathwohl, G. and Liu, T., Crack resistance and fatigue of transforming ceramics: I, materials in the ZrO_2–Y_2O_3–Al_2O_3 system. *J. Am. Ceram. Soc.*, 1991, **74**, 318–325.